Histol Histopathol (2012) 27: 1459-1470
DOI: 10.14670/HH-27.1459

http://www.hh.um.es

Histology and Histopathology
Cellular and Molecular Biology

Distribution of exogenous metallothionein following intraperitoneal and intramuscular injection of metallothionein-deficient mice

Katherine E. Lewis, Roger S. Chung, Adrian K. West and Meng Inn Chuah
Menzies Research Institute Tasmania, University of Tasmania, Hobart, Tasmania, Australia

Summary. Metallothionein-I/II (MT-I/II) is a small metal-binding protein with antioxidant and neuroprotective properties, which has been used experimentally as a neurotherapeutic agent in multiple conditions. Therefore it is important to determine whether exogenous MT-I/II is retained in specific organs or expelled from the body following intramuscular and intraperitoneal injection. The distribution of exogenous MT-IIA (the major human MT-I/II isoform) was examined in MT-I/II-deficient mice, by immunohistochemistry of tissue samples and western blotting of urine samples. MT-IIA was detected within epithelial cells of the kidney cortical and medullary tubules within 1 hour of either intramuscular or intraperitoneal injection. Additionally, MT-IIA was detected within the urine at 1 hour after injection, indicating rapid absorbance into the circulation and filtration through the kidney glomerulus. A portion of the intramuscularly-injected MT-IIA remained within the muscle for at least 24 hours after injection. No MT-IIA was observed within the liver or the brain after either a single injection or a series of MT-IIA injections. These results are consistent with earlier reports that exogenously administered MT-IIA does not cross the intact blood-brain barrier, although a receptor for MT-I/II (megalin) is present in the choroid plexus. We postulate that due to losses through the urine, circulating MT-IIA levels drop rapidly after injection and do not permit transport across the choroid plexus. Peptide analogues of MT-I/II with similar neuroactive properties (emtins) may be more suited for CNS delivery.

Key words: MT-I/II-knockout mice, MT-IIA injection, Urinary system, Liver, Brain

Offprint requests to: Meng Inn Chuah, Menzies Research Institute Tasmania, University of Tasmania, 17 Liverpool Street, Hobart, Tasmania, Australia 7001. e-mail: Inn.Chuah@utas.edu.au

Introduction

Metallothionein (MT) proteins are a family of small cysteine-rich metal-binding proteins, first isolated from horse kidney (Kagi and Vallee, 1960). MT gene expression is modulated by the presence of metal ions (Hamer, 1986), glucocorticoids (Richards et al., 1984), oxidative stress (Feng et al., 2006), and cytokine levels (Cousins and Leinart, 1988). There are four mammalian isoforms of metallothionein (MT-I to MT-IV). The MT-I and MT-II isoforms are almost identical in their structure and expression profile, and are often treated as a single isoform (referred to as MT-I/II) (Penkowa et al., 1999; Chung et al., 2003). Due to its metal-binding properties, MT-I/II is thought to play some role in normal metal homeostasis and in protection from heavy metal toxicity (Michalska and Choo, 1993; Masters et al., 1994). The high cysteine residue content (30%) of MT-I/II confers potent antioxidant properties both *in vitro* (Thornalley and Vasák, 1985; Abel and de Ruiter, 1989) and *in vivo* (Kang et al., 1999).

MT-I/II also displays neuroprotective properties, with increased levels of MT-I/II associated with neural protection during focal cerebral ischaemia (Campagne et al., 1999; Trendelenburg et al., 2002), and with decreased tissue damage after traumatic brain injury (Penkowa et al., 1999; Giralt et al., 2002a,b). MT-I/II is able to promote neuronal growth and regeneration after scratch injury *in vitro*, and after focal brain injury *in vivo* (Chung et al., 2003; Fitzgerald et al., 2007). MT-I/II is upregulated and secreted by astrocytes in response to neuronal injury (Chung et al., 2004); binds to and is internalised into neurons via the endocytic receptor megalin (LRP2) (Chung et al., 2008); and activates multiple protein kinase pathways leading to neurite growth (Ambjorn et al., 2008; Asmussen et al., 2009b).

MT-I/II is suggested to have a neuroprotective function in neurodegenerative diseases such as

Alzheimer's disease (Hidalgo et al., 2006), Parkinson's disease (Ebadi and Sharma, 2006) and amyotrophic lateral sclerosis (Nagano et al., 2001). The protective and regenerative functions of MT-I/II make it a potentially useful neurotherapeutic agent. Recent studies have reported that intraperitoneally-administered MT-I/II entered the central nervous system (CNS) when the blood-brain barrier (BBB) was damaged by induction of EAE (Penkowa and Hidalgo, 2000) or traumatic brain lesion (Giralt et al., 2002a), but was not able to cross the intact BBB.

MT-IIA protein is the major human isoform of MT-I/II. This study aims to investigate the biodistribution of exogenously administered MT-IIA following either a single injection, or once-daily injections over a three-day period. MT-IIA protein was injected into MT-I/II-deficient mice and its presence or absence within the brain, liver, kidneys, urine and injected muscle was determined. MT-I/II-deficient mice were used to ensure that any immunoreactivity detected was due to the presence of exogenously administered MT-IIA rather than endogenous mouse MT-I/II proteins. We found that some MT-IIA rapidly entered the circulation following injection, although a portion remained within the injected muscle. MT-IIA was localised to the kidney, and also found in urine samples, shortly after administration. MT-IIA was not observed within the liver or brain parenchyma, and may be effectively lost through the kidneys.

Materials and methods

Animals

All procedures involving animals were approved by the Animal Ethics Committee of the University of Tasmania (A10230), and were conducted in accordance with the Australian Code of Practice for the Care and Use of Animals for Scientific Purposes. All efforts were made to minimise animal suffering, with injected volumes kept to a minimum, and perfusion performed under sodium pentobarbitone anaesthesia. Animals were maintained in standard housing conditions with a 12 hour light/dark cycle, and received food and water *ad libitum* throughout the study.

The mice used for this study lack functional MT-I and MT-II proteins and are referred to as MT-I/II-knockout (or 'MTKO') mice. The MTKO mice are maintained as homozygotes on a 129Sv genetic background and produce mutant mRNA from the *MT-I* and *MT-II* genes, which both contain an in-frame stop codon (Masters et al., 1994). MTKO mice appear phenotypically normal under standard laboratory conditions, but are more susceptible to heavy metal toxicity than their wild type littermate (Masters et al. 1994) and display decreased wound healing after neural injury (Giralt et al. 2002a).

Administration of exogenous metallothionein

MT-IIA is the predominant human isoform of MT-I/II. Purified rabbit liver Zn_7-MT-IIA (Bestenbalt, Estonia) was dissolved in sterile 0.9% saline for injection (hereafter referred to as MT-IIA). Solubility in saline varied between Zn_7-MT-IIA batches and in some cases a small amount of NaOH was added to aid dissolution. MT-IIA in saline was administered to MTKO mice either via intraperitoneal (i.p.) injection, or via unilateral intramuscular (i.m.) injection into the gastrocnemius or posterior thigh muscle group. MTKO mice received MT-IIA doses in accordance with one of three injection schedules listed in Fig. 1 (Fig. 1a-c), with each injection giving a dose of 10mg Zn_7-MT-IIA per kilogram body weight.

Nine mice were sacrificed for analysis shortly after MT-IIA injection – either at 15 minutes after a single i.m. injection (Fig. 1a; n=3), or at 1 hour after a single i.m. or i.p. injection (Fig. 1b; n=3 for each administration route). Six mice received repeated MT-IIA injections at 0, 24 and 48 hours, and were sacrificed at 72 hours (24 hours after the third MT-IIA injection) to examine MT-IIA accumulation (Fig. 1c; n=3 for each administration route). One age-matched control MTKO mouse was sacrificed for analysis at 1 hour after a single intramuscular injection of saline. A single saline-injected control animal was sufficient to verify that the anti-MT-I/II antibody used in this study did not return a positive result for MT-I/II proteins in the MTKO mice. At the appropriate time point after injection (Fig. 1), mice were deeply anaesthetised with an overdose of sodium pentobarbitone (50 mg/kg) and transcardially perfused with phosphate-buffered saline, pH 7.4 (PBS). Tissue

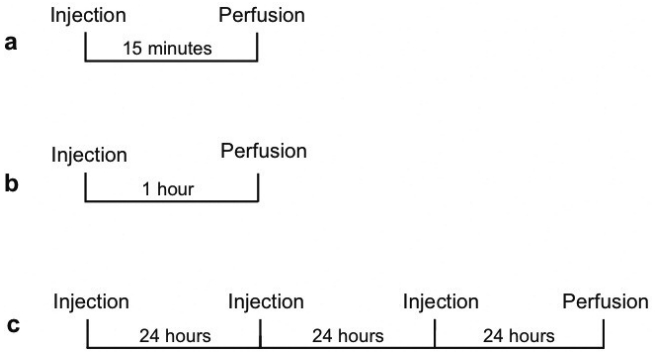

Fig. 1. Schedule for injection of MT-IIA into MTKO mice. Intramuscular injection of MT-IIA and perfusion at 15 minutes post-injection (**a**, n=3). Intramuscular or intraperitoneal injection of MT-IIA and perfusion at 1 hour post-injection (**b**, n=3 intramuscular, n=3 intraperitoneal). Repeated intramuscular or intraperitoneal injections of MT-IIA at 0, 24 and 48 hours, followed by perfusion at 72 hours (**c**, n=3 intramuscular, n=3 intraperitoneal).

samples for immunohistochemistry were dissected from the brain, liver, kidney, injected hindlimb muscle and contralateral hindlimb muscle, and post-fixed in 4% paraformaldehyde overnight at 4°C. Urine samples were extracted from the urinary bladder during dissection, and stored at -20°C for analysis by western blot. Paraformaldehyde-fixed tissues were dehydrated and embedded in paraffin, then five-micron sections were cut on a microtome (Microm), and were mounted on 3-aminopropyltriethoxysilane-coated slides.

Anti-MT-I/II antibody

Injected MT-IIA protein was detected by tissue immunohistochemistry and urine sample western blotting, using a mouse monoclonal antibody against MT-I/II protein (anti-MT-I/II, clone E9, Dako, Carpinteria, CA). This antibody detects all known isoforms of the MT-I/II protein, but does not cross-react with MT-III or MT-IV protein. Using this antibody in conjunction with MTKO mice, any MT-I/II-immunoreactivity detected following MT-IIA injection can be attributed to the exogenously administered MT-IIA.

Immunohistochemistry for MT-I/II

Paraffin-embedded sections were dewaxed, rehydrated through graded alcohols to distilled water, and rinsed in PBS. Endogenous peroxidases were quenched with 10-minute incubation with 3% hydrogen peroxide in PBS. A Mouse on Mouse (M.O.M) kit (Vector Laboratories, Burlingame, CA) was used according to the manufacturer's instructions, to minimise secondary antibody interactions with the tissue. Briefly, sections were blocked by application of M.O.M blocking reagent for 1 hour, then washed in PBS and incubated with M.O.M antibody diluent for 5 minutes. Anti-MT-I/II primary antibody was applied to the sections for 30 minutes (1:1000 in M.O.M antibody diluent). M.O.M kit biotinylated anti-mouse secondary antibody was subsequently applied for 10 minutes (1:250 in M.O.M antibody diluent). The biotin label was detected by horseradish-peroxidase (HRP)-conjugated streptavidin, applied to the sections for 30 minutes (Dako, Carpinteria, CA), and by application of 3,3-diamino-benzidine (DAB) substrate for 5 minutes (Vector Laboratories, Burlingame, CA). Upon reaction with HRP, DAB forms an insoluble brown precipitate at the sites of positive immunoreactivity. Slides were counterstained by immersion in Mayer's haematoxylin, dehydrated through graded alcohols and xylene, and mounted in permanent mounting medium. The slides were examined using a Leica DM2500 light microscope, and images were captured using a Leica DFC495 camera. The white balance for each image was adjusted with Adobe Photoshop CS5, using unobstructed transmitted light as a common reference point (as seen through lumens and capillaries in each section).

Western blotting

The presence of MT-IIA in MTKO mouse post-injection urine samples was assessed using the NuPAGE western blot system (Invitrogen, Carlsbad, CA) according to the manufacturer's instructions, with minor modifications. Briefly, each urine sample was diluted 1:2 with sterile distilled water; 21 μl of diluted sample was then mixed with 7 μl reducing sample buffer (10% ß-mercaptoethanol (Sigma) in NuPAGE LDS Sample Buffer) and heated to 95°C for 5 minutes. Samples were spun briefly and loaded onto a NuPAGE precast 10% bis-tris polyacrylamide gel. A protein ladder was included on each gel (NuPAGE See Blue Plus2 prestained standards). The gel was electrophoresed at 200V for 30 minutes using NuPAGE MES Running Buffer, with NuPAGE Antioxidant used to maintain reducing conditions. The proteins were transferred to a nitrocellulose membrane at 30V for 60 minutes, using Towbin transfer buffer composed of 192mM glycine, 25mM trizma base, 20% v/v methanol in distilled water. The membrane was blocked with 5% non-fat milk powder in PBS with 0.05% Tween-20 added (5% MP/PBST) overnight at 4°C; then the antibody incubation steps were performed at room temperature. The membrane was incubated with anti-MT-I/II for 1 hour (1:1000 in 2.5% MP/PBST), biotinylated goat anti-mouse- for 1 hour (Dako, Carpinteria, CA; 1:1000 in 2.5% MP/PBST), and HRP-conjugated streptavidin for 1 hour (BioSource, Camarillo, CA; 1:5000 in 2.5% MP/PBST), with three 5-minute washes in PBS-T between each step. Antibodies bound to the membrane were detected by ECL using SuperSignal West Dura Substrate (Thermo Scientific, Waltham, MA), and visualised using the Vilber Lourmat ChemiSmart 5000 Gel Documentation System. Using Adobe Illustrator CS5, the western blot image was inverted and the protein ladder was overlaid. Band size was estimated by comparison with the protein ladder. The western blot was not quantitated by band intensity due to the presence of oversaturated pixels in some images, and also due to the absence of a protein in the urine which could be reliably used as a loading control. Therefore the results from the western blots cannot compare the amount of MT-IIA between samples, and reveals only the presence or absence of MT-IIA in the urine.

Results

MT-I/II-immunoreactivity is observed in the injected muscle after both single and repeated injections

MT-I/II-immunoreactivity was observed within the injected hindlimb muscle at 15 minutes after intramuscular injection (Fig. 2a) and at 1 hour after intramuscular injection (Fig. 2b,c). Near the injection site, MT-I/II-immunoreactivity was localised within the muscle fibres at both 15 minutes and 1 hour after i.m. injection (Fig. 2a,b). Further from the injection site, MT-

I/II-immunoreactivity was only sparsely observed within muscle fibres, and was also observed in capillaries running between fibre bundles (Fig. 2c). Endothelial cells of a large blood vessel within the injected muscle also showed positive immunoreactivity for MT-I/II at 15 minutes post-injection (Fig. 2f), indicating that MT-IIA rapidly entered the vascular system after i.m. injection.

MT-I/II-immunoreactivity was also observed within the injected muscle at 24 hours after the third of three i.m. MT-IIA injections (Fig. 2d), indicating that some injected MT-IIA had remained within the injected muscle for at least 24 hours following i.m. injection. No MT-IIA was detected within saline-injected hindlimb muscle (Fig. 2e), nor in contralateral uninjected hindlimb muscle, or in muscle from mice injected intraperitoneally with MT-IIA (data not shown).

MT-I/II-immunoreactivity is present in the renal cortex and medulla within 1 hour of MT-IIA administration

MT-I/II-immunoreactivity was detected in proximal tubules of the kidney cortex at 15 minutes and at 1 hour after i.m. injection, and at 1 hour after i.p. injection (Fig. 3a-c). At both 15 minutes and 1 hour after injection, punctate MT-I/II-immunoreactivity was observed within the apical region of the cuboidal cells comprising the proximal tubule epithelium (Fig. 3a-c). The punctate pattern of staining at the apical membrane suggests uptake of MT-IIA from the proximal tubule lumen into epithelial cells by endocytosis, forming MT-I/II-positive vesicular structures. No MT-I/II-immunoreactivity was observed in the renal cortex 24 hours after the last of three MT-IIA injections administered either i.p. (Fig. 3d) or i.m. (Fig. 3e). No immunoreactivity for MT-I/II was detected after saline injection (Fig. 3f).

MT-I/II-immunoreactivity was observed within the renal medulla at 1 hour after i.p. and i.m. injection (Fig. 4). No MT-I/II-immunoreactivity could be detected in the medulla at either 15 minutes after i.m. injection, or 24 hours after the last of three MT-IIA injections. Within both the outer and inner stripes of the outer medulla (see schematic diagram Fig. 4a), MT-I/II-immunoreactivity formed a diffuse cytoplasmic pattern in squamous epithelial cells at 1 hour after i.m. injection (Fig. 4d,e), but not after i.p. injection (Fig. 4b). MT-I/II-immunoreactivity was also present within some cuboidal

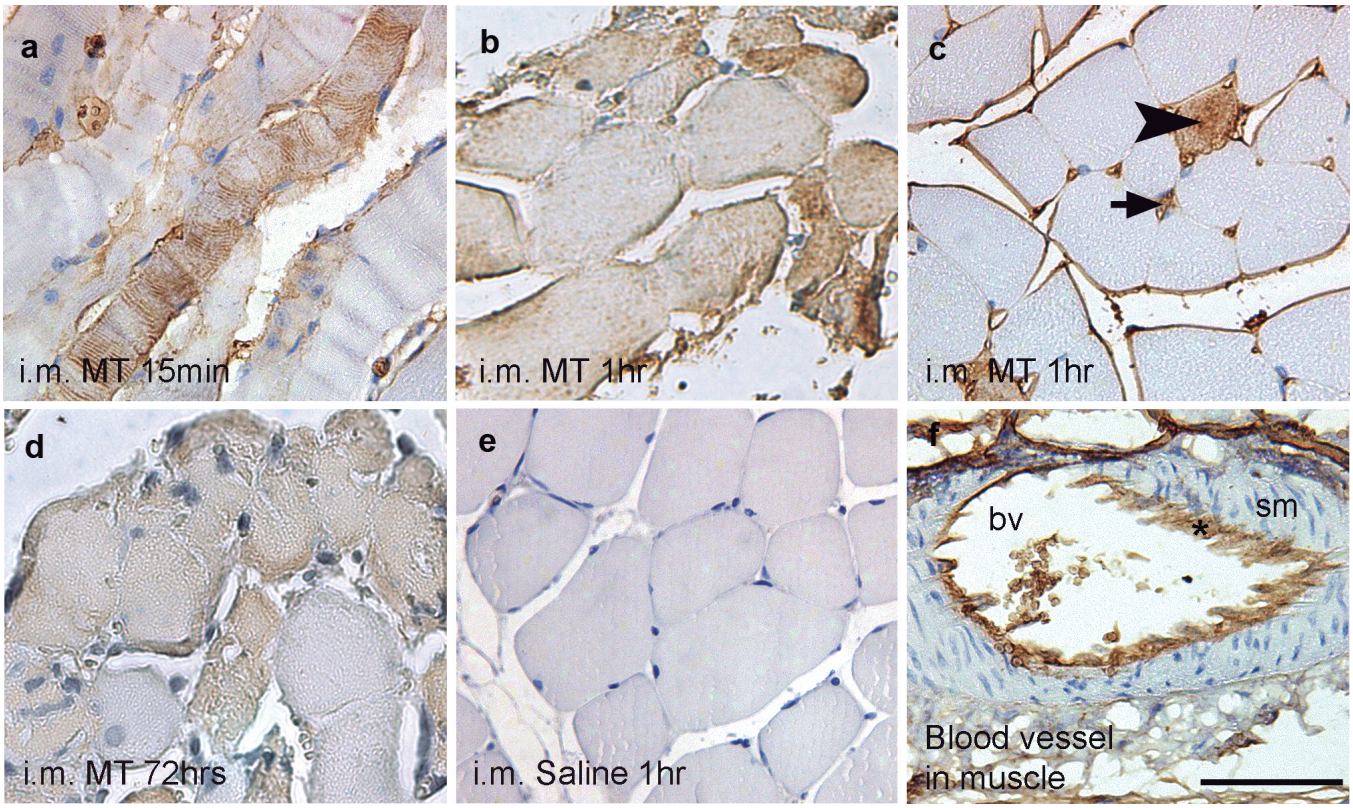

Fig. 2. Localisation of MT-IIA within hindlimb skeletal muscle following intramuscular injection. MT-I/II-immunoreactivity can be seen within muscle fibres near the injection site at 15 minutes post-injection **(a)** and 1 hour post-injection **(b)**; and at 72 hours, following repeated i.m. injections **(d)**. MT-I/II-immunoreactivity is also seen within muscle fibres (**c**, arrowhead) and in small blood vessels (**c**, arrow) some distance from the injection site, at 1 hour post-injection. Saline-injected MTKO muscle shows no immunoreactivity for MT-I/II **(e)**. MT-I/II-immunoreactivity is seen within the endothelium of a large blood vessel within the injected muscle at 15 minutes after i.m. injection (**f**, asterisk). sm: smooth muscle; bv: blood vessel. Scale bar: a-e, 50 μm; f, 100 μm.

epithelial cells of collecting ducts in the inner medulla, at 1 hour after i.m. or i.p. injection (Fig. 4c,f). The cuboidal cells of the collecting duct displayed a mixture of MT-I/II-positive and MT-I/II-negative cells (seen in Fig. 4c,f), suggesting selective uptake of MT-IIA by one of the two cell types comprising the collecting duct (Kierszenbaum, 2007). Again, no MT-I/II-immunoreactivity was seen in the renal medulla following saline injection (Fig. 4g-i).

MT-IIA is present in the urine shortly after injection

The presence of MT-IIA in urine samples was determined using western blotting. A spare aliquot of the injected MT-IIA solution was run on each western blot as a positive control, and gave a single band at 7kDa molecular weight (as seen in Fig. 5a, lane 9). A band at 7kDa, denoting MT-IIA, was present in urine samples taken within 1 hour of MT-IIA injection (Fig. 5a), but was not present in samples taken at the 72 hour timepoint (i.e. 24 hours after the last of three injections) (Fig. 5b). A weak MT-IIA band was present in one of the two samples collected at 15 minutes after i.m. injection (no urine was able to be collected from the third mouse perfused at this time point) (Fig. 5a, lanes 1-2). A stronger MT-IIA band was detected in all three samples collected at 1 hour after i.m. injection; and in two of the three samples collected at 1 hour after i.p. injection (Fig. 5a, lanes 3-8).

Some high-molecular-weight bands were observed in all urine samples, including the sample taken after saline injection (Fig. 5c), indicating some non-specific binding to proteins within the urine. These bands were also observed in the absence of primary antibody (data not shown) – it is possible that there are endogenous mouse immunoglobulin fragments within the urine samples, which are unintentional targets for the anti-mouse secondary antibody employed in the western blot procedure. However, none of the samples showed any bands of molecular weight <25kDa when the primary antibody was omitted, and urine from the saline-injected MTKO mouse did not show any bands below 25kDa when probed with the primary antibody (see Fig. 5c). We can therefore surmise that the band at 7kDa observed in urine from 1 hour post-injection was due to specific binding of the primary antibody to MT-IIA within the

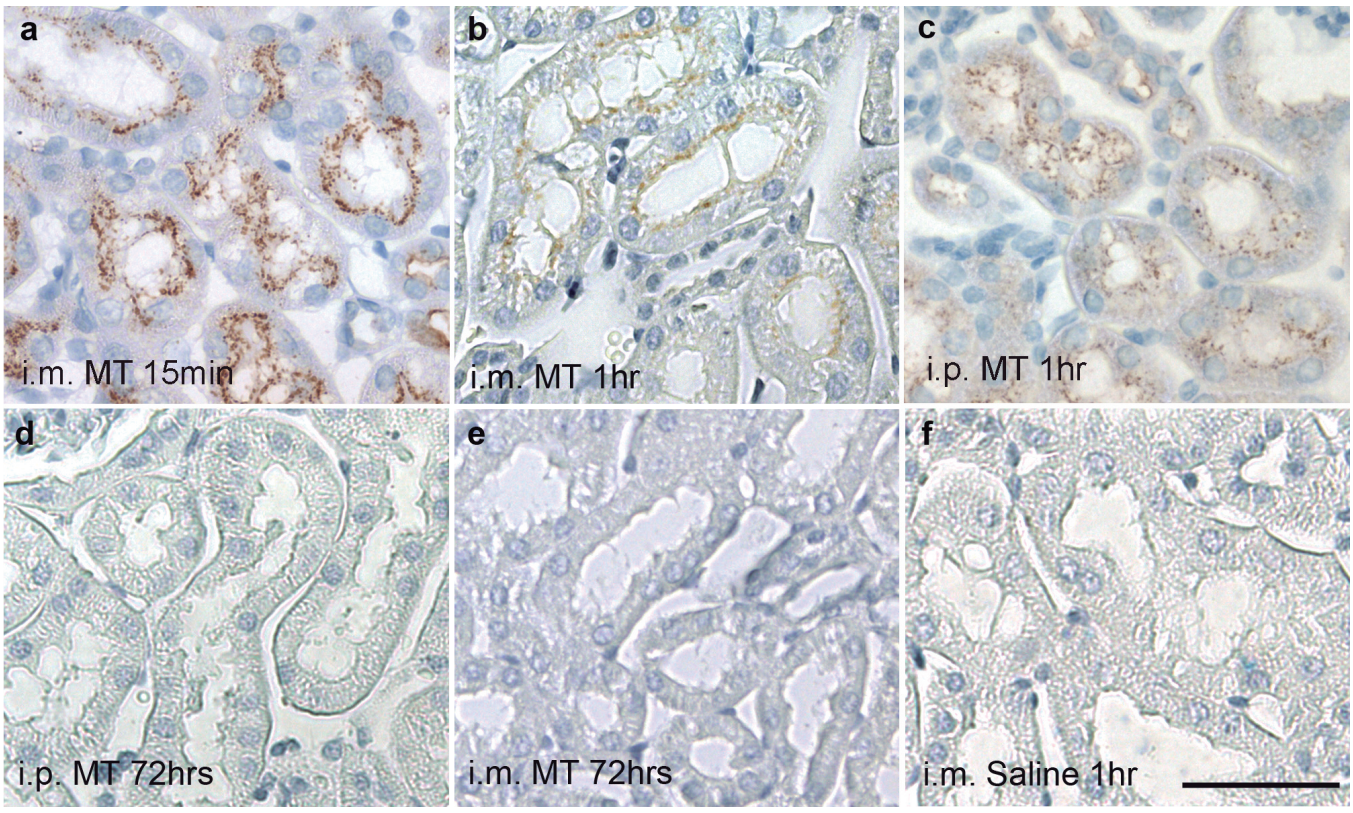

Fig. 3. Localisation of MT-IIA within the renal cortex following intraperitoneal or intramuscular injection. MT-I/II-immunoreactivity forms a punctuate staining pattern within the epithelial cells of the cortical proximal convoluted tubules at 15 minutes after intramuscular injection **(a)**, and at 1 hour after intramuscular or intraperitoneal injection (**b** and **c,** respectively). No MT-I/II-immunoreactivity is observed within the cortical tubules at 72 hours, after three intramuscular or intraperitoneal injections of MT-IIA **(d, e)**. Similarly, no MT-I/II-immunoreactivity is seen in the kidney cortex after saline injection **(f)**. Scale bar: 50 μm.

urine sample. The presence of MT-IIA in urine collected within 1 hour of injection indicates that MT-IIA was rapidly lost through the kidneys after injection.

To examine whether this loss of MT-IIA in the urine was specific to MTKO mice, we injected two age- and background-matched wild type mice with either MT-IIA or saline, and collected urine samples at 1 hour post-injection. The wild type mouse receiving saline showed no positive MT-IIA band by western blot, while the wild type mouse receiving intramuscular MT-IIA showed an

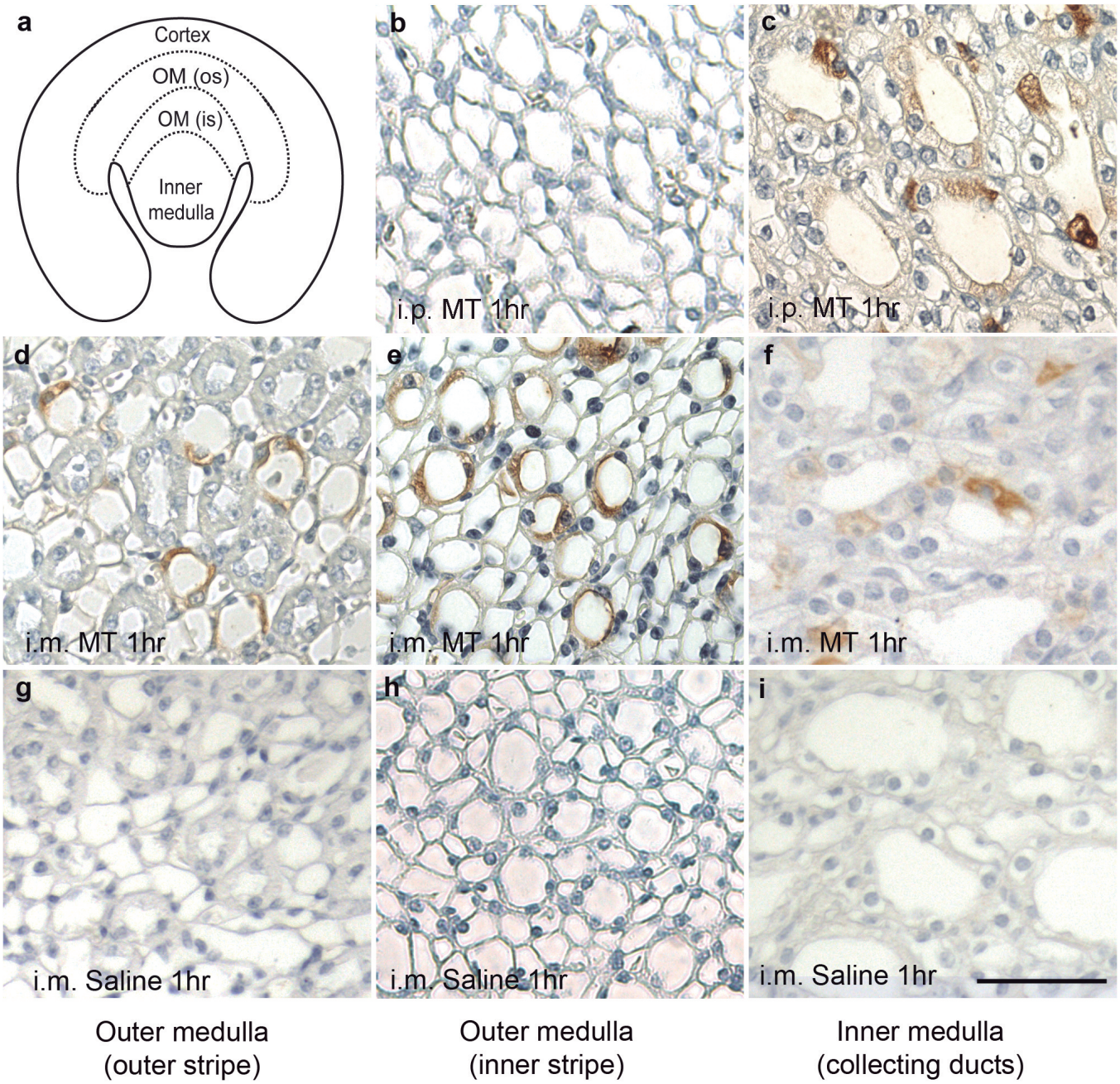

Fig. 4. Localisation of MT-IIA within the renal medulla following intraperitoneal or intramuscular injection. Images in this figure were acquired within the regions indicated on the schematic diagram **(a)** – outer stripe of the outer medulla **(d, g)**, inner stripe of the outer medulla **(b, e, h)**, and inner medulla **(c, f, i)** containing collecting ducts. MT-I/II-immunoreactivity is observed in a cytoplasmic distribution within squamous epithelia in the outer medulla at 1 hour after intramuscular injection (**d** and **e**, respectively), but this pattern was not observed after intraperitoneal injection **(b)**. MT-I/II-immunoreactivity is seen in the collecting duct epithelial cells at 1 hour after either intramuscular or intraperitoneal injection **(c, f)**. No MT-I/II-immunoreactivity can be detected within the medulla after saline injection **(g-i)**. OM: outer medulla; os: outer stripe; is: inner stripe. Scale bar: 50 μm.

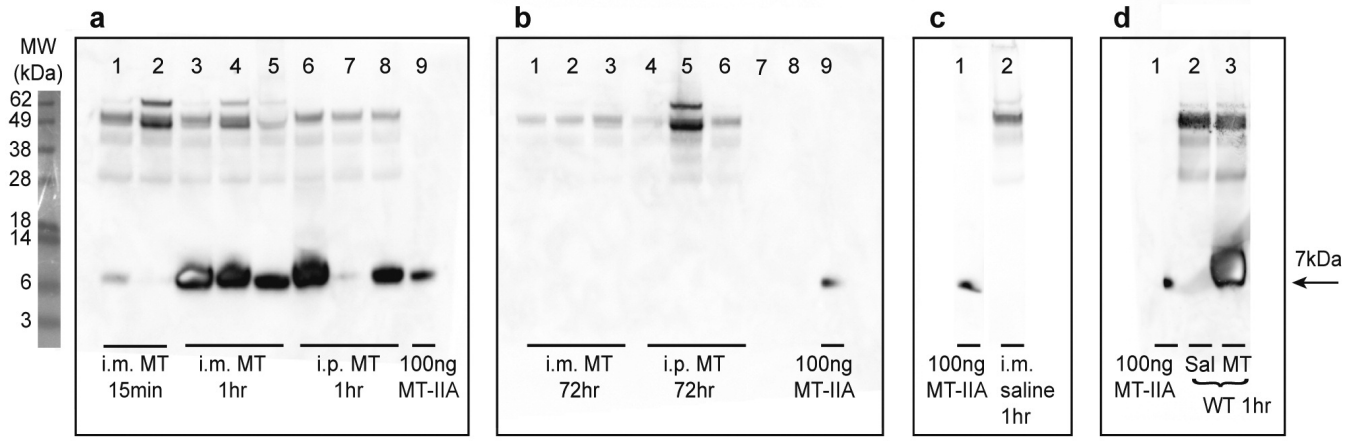

Fig. 5. Presence of MT-IIA in urine samples following injection. MT-IIA was detected in the urine of MTKO mice within 1 hour of MT-IIA injection. 100 ng of purified MT-IIA dissolved in distilled water shows a single band at 7kDa (**a and b**, lane 9; **c and d**, lane 1). Positive bands for MT-IIA were observed in urine samples from 15 minutes and 1 hour post-i.m. injection (**a**, lanes 1-5) and from 1 hour post-i.p. injection (**a**, lanes 6-8). No bands for MT-IIA were detected at the 72-hour timepoint, after repeated i.m. or i.p. injections **(b)**. Urine from a saline-injected MTKO mouse shows three bands caused by non-specific binding of the secondary antibody at approximately 55kDa, 45kDa and 30kDa (**c**, lane 2). All other urine samples also show various amounts of these nonspecific bands. Urine from one MT-IIA-injected wild type mouse also shows a MT-IIA band at 7kDa (**d**, lane 3) which is absent from the urine of a saline-injected wild type mouse (**d**, lane 2).

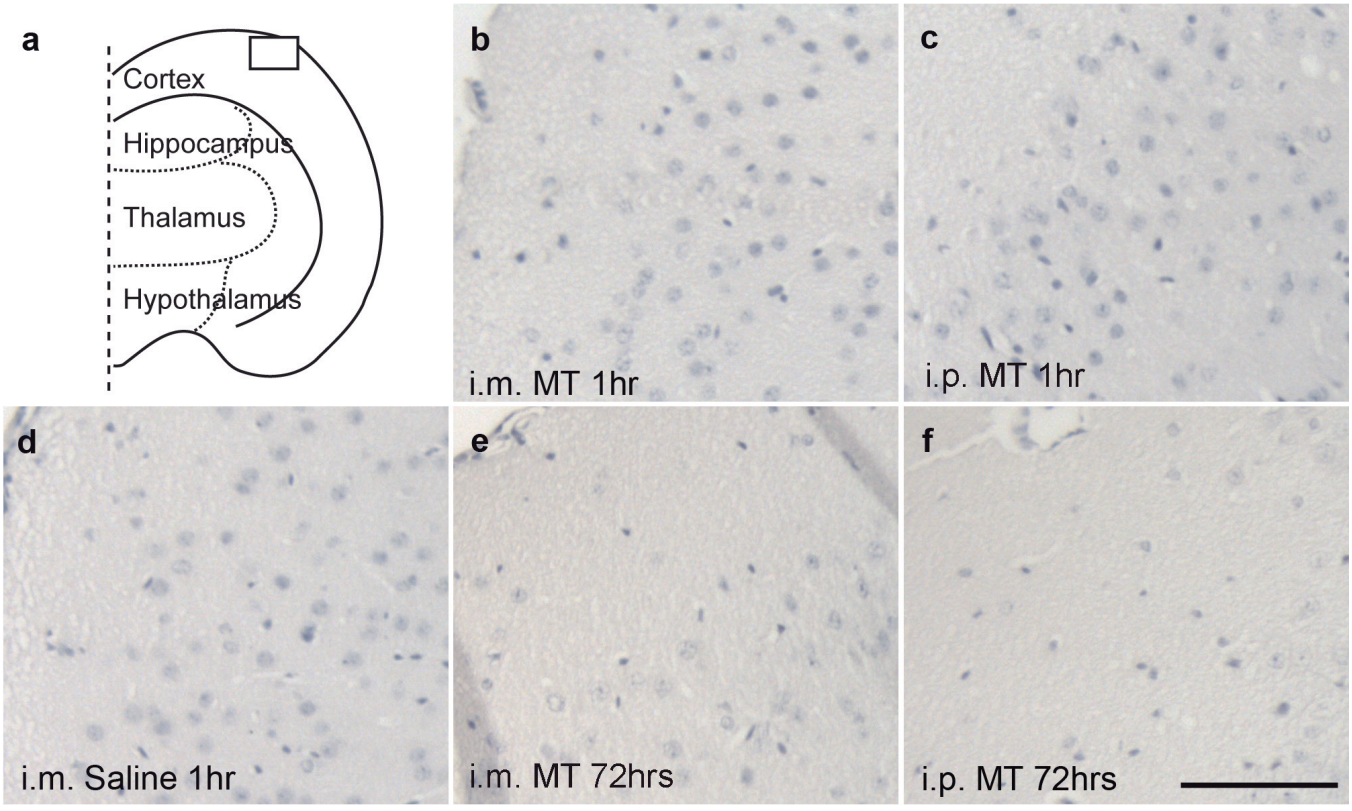

Fig. 6. MT-IIA is not localised to the brain after i.m. or i.p. injection. Schematic diagram **(a)** shows some of the areas examined in coronal brain sections. Images presented in this figure are taken from the cerebral cortex (**a**, rectangle; not to scale). No MT-I/II-immunoreactivity was observed within the grey matter of the cerebral cortex at 1 hour after i.p. or i.m. injection **(b, c)**, nor after saline injection **(d)** or after repeated i.p. or i.m. injections **(e, f)**. Scale bar: 50 μm.

intense band at approximately 7kDa (Fig. 5d). These data suggest that the loss of MT-IIA in the urine is not specific to MTKO mice.

MT-IIA is not delivered to the brain or the liver via intramuscular or intraperitoneal administration

The brain was examined in coronal sections (represented in schematic diagram as shown in Fig. 6a). No MT-I/II-immunoreactivity was observed within the grey matter of the brain cerebral cortex after a single i.m. or i.p. MT-IIA injection (Fig. 6b,c). Similarly, no MT-I/II-immunoreactivity was observed after saline injection (Fig. 6d) or after repeated i.m. or i.p. MT-IIA injections (Fig. 6e,f). No immunoreactivity was seen in any other area of the brain examined, including the white matter, hippocampus, thalamus, midbrain or cerebellum (data not shown; absence of immunoreactivity in these areas is similar to that seen in grey matter images shown in Fig. 6b-f). Additionally, no MT-I/II-immunoreactivity could be detected within the liver parenchyma at any of the analysed timepoints, after either i.p. or i.m. administration (Fig. 7a-e). These results indicate that the injected MT-IIA was not readily taken up into the brain or the liver from the bloodstream; and also indicate that MT-IIA does not appear to have accumulated in these organs following repeated injections.

Discussion

MT-IIA is capable of rapidly entering the bloodstream after injection, although some remains within the injected muscle

Our results show that MT-IIA rapidly enters the bloodstream after either i.m. or i.p. injection. MT-IIA-positive capillaries and large blood vessels were observed within 1 hour after i.m. injection (Fig. 2). MT-IIA was seen in the cortical and medullary kidney tubules at 1 hour after injection via either delivery route (Figs. 3, 4), indicating that MT-IIA enters the circulation and travels to the kidney within 1 hour of injection. However, not all MT-IIA was absorbed from the injection site following intramuscular injection. MT-IIA was detected within the injected muscle at both 15 minutes and 1 hour after injection (Fig. 2), indicating that a portion of the injected MT-IIA is not immediately absorbed into the circulation. Unexpectedly, some MT-

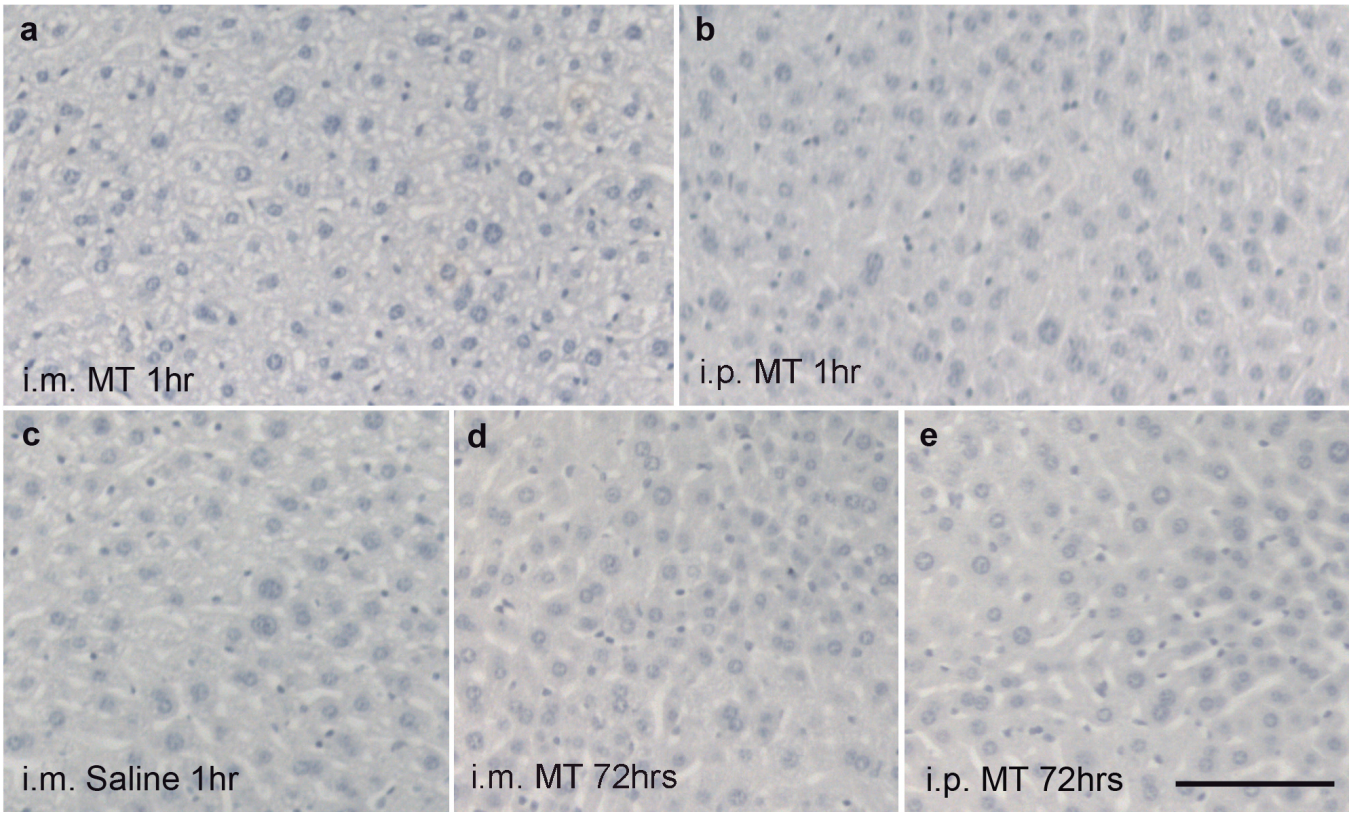

Fig. 7. MT-IIA is not localised to the liver after i.m. or i.p. injection. No MT-I/II-immunoreactivity was observed within the liver at 1 hour after a single MT-IIA injection **(a,b)**, after repeated MT-IIA injections **(d,e)** or after saline injection **(c)**. Scale bar: 100 μm.

IIA was still detectable within the injected muscle at 24 hours after the last of three repeated injections (Fig. 2d). No MT-IIA was detected within the muscle of mice injected i.p. with MT-IIA, indicating that MT-IIA does not accumulate in the muscle even if present within the circulation. This indicates that some portion of the injected MT-IIA remains within the injected muscle for at least 24 hours after injection. It is unclear whether the remaining intramuscular MT-IIA would eventually be degraded, or would be released into the systemic circulation.

MT-IIA is taken up by epithelial cells in the renal tubules

In this study, MT-IIA was observed in epithelial cells in both the cortical and medullary kidney regions (Figs. 3, 4) within 1 hour of i.m. or i.p. injection. MT-IIA is a small protein (7kDa), and its rapid appearance in the kidneys after injection indicates fast absorption from the injection site into the systemic circulation, and filtration through the glomerulus into the nephron lumen. The punctate pattern of immunoreactivity within cortical proximal tubule cells, and the localisation of those puncta to the region of cytoplasm near the apical membrane, indicates that MT-IIA could have been reabsorbed from the lumen of the nephron by endocytosis. This is consistent with previous reports showing that cadmium- or lead-complexed MT-I/II protein can be internalised at the apical surface of proximal tubule cells by the endocytic receptor protein, megalin (Klassen et al., 2004; Wolff et al., 2006). Megalin, or low density lipoprotein receptor-related protein 2 (LRP2), is a multiligand receptor belonging to the LDL receptor superfamily which plays an essential role in reuptake of filtered plasma proteins in the proximal tubule (Christensen et al., 1998; Leheste et al., 1999; Verroust and Christensen, 2002). Zinc-complexed MT-I/II has been shown previously to interact with and be internalised by megalin at the membrane of cultured neurons (Fitzgerald et al., 2007; Chung et al., 2008). It is therefore likely that in this study, the observed uptake of zinc-complexed MT-IIA into proximal tubule cells is due to megalin-mediated endocytosis.

MT-IIA was also observed in epithelial cells within the renal medulla at 1 hour after injection (Fig. 4). Within both the inner and outer stripes of the outer medulla, MT-IIA was seen in a diffuse pattern within squamous epithelial cells (Fig. 4). There are two structures with a squamous epithelium within this kidney region – the thin limb of the loop of Henle, and the vasa recta (Kierszenbaum, 2007). The vasa recta capillary network runs parallel to the loop of Henle, creating a counter-current arrangement for reabsorption of salts and water, and the two tubules are structurally difficult to distinguish (Kierszenbaum, 2007). The uniform circular shape and marginally thicker epithelium of the MT-IIA-positive tubules tentatively identify these tubules as the thin limb of the loop of Henle, rather than the vasa recta. However, the loop of Henle is not known to be involved in protein reabsorption or secretion, and there are no reports of LDL receptor superfamily member expression in the thin limb of the loop of Henle. It is unclear how MT-IIA would be absorbed into these epithelial cells. The MT-IIA distribution is cytoplasmic rather than punctuate, indicating that MT-IIA may be rapidly released into the cytoplasm after endocytic uptake, or may be absorbed into the cells by a mechanism other than endocytosis. It is possible that there is an as-yet uncharacterised transport mechanism for MT-IIA within the epithelial cells of the loop of Henle thin limb.

Within the inner medulla, MT-IIA was detected within the cuboidal epithelial cells of the collecting duct at 1 hour after i.m. and i.p. (Fig. 4) injection. MT-IIA appears to be selectively taken up by only some of the cells comprising the collecting duct (Kierszenbaum, 2007), although the two cell types present in the collecting duct – principal cells and intercalated cells – cannot be distinguished through light microscopy alone. Due to the reported paucity of intercalated cells previously observed within rodent inner medullary collecting ducts (Clapp et al., 1987), the MT-IIA-positive cells are likely to be a subset of principal cells. The distribution of MT-IIA within collecting duct cells appears cytoplasmic and somewhat granular, indicating that MT-IIA could be present, at least in part, within vesicular structures.

Although megalin is not expressed in the collecting duct, another member of the LDL receptor superfamily (known as sorLA/LR11) is present within collecting duct cells (Riedel et al., 2002). Within collecting duct principal cells and a subset of intercalated cells, sorLA/LR11 is reported to be localised to the intracellular trafficking structures, including cytoplasmic vesicles and the Golgi network, but was not observed at the cell membrane (Riedel et al., 2002). SorLA/LR11 displays some sequence and domain homology with the related transmembrane endocytic receptor LRP1; can bind to some of the same ligands as LRP1; and interacts with LRP1 in cell culture systems (Spoeglen et al., 2009). Similarly to both LRP1 and megalin, sorLA/LR11 can mediate endocytosis of apolipoprotein ligands if expressed at the cell membrane *in vitro* (Nilsson et al., 2008). As MT-IIA associates with both LRP1 and megalin (Ambjorn et al., 2008), it is possible that MT-IIA might also be a ligand of sorLA/LR11. We speculate that if sorLA/LR11 were capable of shuttling between both intracellular and membrane compartments, this may provide an opportunity for the internalisation of ligands such as MT-IIA, and could explain the apparent uptake of MT-IIA into collecting duct epithelial cells in this study.

The fate of the reabsorbed MT-IIA is as yet undetermined. The typical pathway of LDL-receptor-mediated uptake was thought to end in lysosomal degradation of the protein (Christensen and Nielsen, 1991). More recent studies have shown that this may not always be the case – both megalin and the LDL-receptor are both capable of transcytosis of intact proteins across

epithelial cells (Zlokovic et al., 1996; Dehouck et al., 1997; Marino et al., 2001). It is therefore possible that MT-IIA, internalised into proximal tubule cells by megalin, may undergo transcytosis to be recycled into the circulation rather than be degraded by lysosomes.

Injected MT-IIA is lost through the kidneys in the urine

MT-IIA was observed in urine at 1 hour after a single i.m. injection, but not in the urine of mice given repeated MT-IIA injections (Fig. 5). The presence of MT-IIA in the urine within 1 hour of injection, again confirms that some injected MT-IIA is rapidly absorbed into the systemic circulation, and filtered into the urine through the glomerulus. While we have demonstrated that some of the MT-IIA is reabsorbed into the tubule epithelial cells, some is also lost through the urine. Saturable reabsorption of cadmium-complexed MT has been previously demonstrated in rabbit kidney (Foulkes, 1978), and the transport systems for MT-IIA which are present within the renal tubule cells (Klassen et al., 2004) of mouse kidney may also be saturated if MT-IIA is present within the lumen at high concentrations.

MT-IIA is not delivered to the liver or CNS by a single injection or by repeated injections

It is clear that MT-IIA rapidly enters the circulatory system after either i.m. or i.p. injection. However MT-IIA does not appear to enter the liver or the brain at 1 hour after any single injection, or after a series of injections over 3 days (Figs. 6, 7), despite its apparent presence within the circulation. This result agrees with previous studies showing that MT-IIA does not cross the intact BBB following i.p. injection (Penkowa et al., 1999; Giralt et al., 2002a). The MT-I/II receptor megalin is reported to be present at the choroid plexus and can mediate transcytosis of its ligands across an *in vitro* model of the blood-brain barrier (Zlokovic et al., 1996; Carro et al., 2005). Additionally, the related LDL receptor is also involved in transcytosis across a blood-brain barrier model (Dehouck et al., 1997). The question therefore remains – if MT-IIA is present in the circulation and megalin expressed at the choroid plexus is capable of mediating transcytosis, why was no MT-IIA takeup into the CNS observed in this study? Similarly, while megalin is not expressed in the liver, another member of the LDL receptor superfamily – low-density-lipoprotein related protein, or LRP1 – is expressed by the liver (Zheng et al., 1994), and has been shown to interact with MT-I/II proteins (Ambjorn et al., 2008). Both LRP1 and megalin are scavenger receptors with many possible ligands (Leheste et al., 1999), so the binding of MT-IIA to megalin or LRP1 may be out-competed by ligands for which the receptors have a higher affinity (Klassen et al., 2005). The entry of MT-IIA into the liver or CNS may therefore depend on the relative serum concentration of MT-IIA versus that of other megalin and LRP1 ligands. It is possible that a single bolus injection of MT-IIA does not maintain the required bloodstream concentration for transcytosis across the blood-brain barrier, due to losses through the kidneys. Additionally, as MT-I/II displays a higher binding affinity for megalin than for LRP1 (Ambjorn et al., 2008), we might speculate that MT-IIA would be detectable in the brain (via megalin-mediated takeup at the choroid plexus) in a higher amount than in the liver (via LRP1-mediated takeup) at a given plasma concentration. However, the immunostaining protocol may not be sensitive enough to detect small amounts of MT-IIA within the brain or liver. A more detailed quantitative study looking at serum MT-IIA levels over time, after a bolus injection versus using continuous infusion, may provide some insight the conditions under which MT-IIA may enter the CNS across the intact blood-brain barrier.

Limitations of the study

One possible reason for the absence of injected MT-IIA in the liver and in the brain may be due to the sensitivity of the immunostaining techniques – even with streptavidin amplification of the signal, small amounts of MT-IIA within these organs may go undetected. It is also possible that MT-IIA in the circulation could be bound to unidentified binding partners, which may prevent its receptor-mediated uptake. The presence of binding partners for MT-IIA within the circulation could also prevent some of the injected dose from clearance through the kidneys into the urine.

Additionally, in the absence of a reliable ELISA for MT-IIA in mouse samples, we have used western blotting to examine the presence or absence of MT-IIA in urine samples. However, this method is not quantitative due to the absence of a loading control protein. There appears to be more MT-IIA in the 1 hour post-injection samples than in the 15 minute post-injection samples (Fig. 5), which could be consistent with rising levels of MT-IIA in the systemic circulation during the first hour after injection. However, quantitation of MT-IIA levels in serum is necessary to properly evaluate the absorption kinetics of any injected MT-I/II protein.

Alternative strategies for delivery of MT-IIA to the CNS

As MT-IIA readily enters the CNS when the BBB is disrupted (Penkowa et al., 1999, Giralt et al. 2002a), systemic delivery of MT-IIA may comprise an appropriate CNS delivery route when the BBB is damaged (depending on how much MT-IIA is lost through the kidneys). For the treatment of neurological conditions in which the BBB is intact, or was previously disrupted and has reformed, an alternative delivery route for MT-IIA must be found. Direct administration into the CNS such as intracerebral, intracerebroventricular and intrathecal infusions bypass the BBB by design, but these are invasive procedures, with substantial

consequences should errors occur during their placement or use. Ideally, MT-IIA could be delivered systemically and taken up into the CNS. The attachment of MT-IIA to an existing BBB transport system, such as the OX26-transferrin receptor complex (Wu and Pardridge, 1999) could be considered, as could manipulation of endogenous megalin levels within the choroid plexus to enhance CNS uptake. Alternatively, the recently-developed emtin peptides are analogues of MT-I/II protein, and are reported to cross the BBB (Sonn et al., 2010). The emtin peptides display similar properties to MT-I/II *in vitro* (Ambjorn et al., 2008; Asmussen et al., 2009a) and provide a promising alternative for MT-IIA protein in the treatment of CNS conditions where the BBB is not disrupted.

Acknowledgements. The authors thank Dr Bill Bennett and Debbie Orchard for assistance in some of the immunostaining procedures. This research was funded by grants from the National Health and Medical Research Council, and the Motor Neurone Disease Research Institute of Australia.

References

Abel J. and de Ruiter N. (1989). Inhibition of hydroxyl-radical-generated DNA degradation by metallothionein. Toxicol. Lett. 47, 191-196.

Ambjorn M., Asmussen J.W., Lindstam M., Gotfryd K., Jacobsen C., Kiselyov V.V., Moestrup S.K., Penkowa M., Bock E. and Berezin V. (2008). Metallothionein and a peptide modeled after metallothionein, EmtinB, induce neuronal differentiation and survival through binding to receptors of the low-density lipoprotein receptor family. J. Neurochem. 104, 21-37.

Asmussen J.W., Ambjorn M., Bock E. and Berezin V. (2009a). Peptides modeled after the alpha-domain of metallothionein induce neurite outgrowth and promote survival of cerebellar granule neurons. Eur. J. Cell Biol. 88, 433-443.

Asmussen J.W., Von Sperling M.L. and Penkowa M. (2009b). Intraneuronal signaling pathways of metallothionein. J. Neurosci. Res. 87, 2926-2936.

Campagne M.v.L., Thibodeaux H., van Bruggen N., Cairns B., Gerlai R., Palmer J.T., Williams S.P. and Lowe D.G. (1999). Evidence for a protective role of metallothionein-1 in focal cerebral ischemia. Proc. Natl. Acad. Sci. USA 96, 12870-12875.

Carro E., Spuch C., Trejo J.L., Antequera D. and Torres-Aleman I. (2005). Choroid plexus megalin is involved in neuroprotection by serum insulin-like growth factor 1. Neurobiol. Dis. 25, 10884-10893.

Christensen E.I. and Nielsen S. (1991). Structural and functional features of protein handling in the renal proximal tubule. In: Seminars in Nephrology. Tisher C. and Madsen W. (eds). WB Saunders Co. Philadelphia. pp. 414-439.

Christensen E.I., Birn H., Verroust P. and Moestrup S.K. (1998). Membrane receptors for endocytosis in the renal proximal tubule. Int. Rev. Cytol. 180, 237-284.

Chung R.S., Vickers J.C., Chuah M.I. and West A.K. (2003). Metallothionein-IIA promotes initial neurite elongation and postinjury reactive neurite growth and facilitates healing after focal cortical brain injury. J. Neurosci. 23, 3336-3342.

Chung R.S., Adlard P.A., Dittmann J., Vickers J.C., Chuah M.I. and West A.K. (2004). Neuron-glia communication: metallothionein expression is specifically up-regulated by astrocytes in response to neuronal injury. J. Neurochem. 88, 454-461.

Chung R.S., Penkowa M., Dittmann J., King C.E., Bartlett C., Asmussen J.W., Hidalgo J., Carrasco J., Leung Y.K., Walker A.K., Fung S.J., Dunlop S.A., Fitzgerald M., Beazley L.D., Chuah M.I., Vickers J.C. and West A.K. (2008). Redefining the role of metallothionein within the injured brain: extracellular metallothioneins play an important role in the astrocyte-neuron response to injury. J. Biol. Chem. 283, 15349-15358.

Clapp W.L., Madsen K.M., Verlander J.W. and Tisher C.C. (1987). Intercalated cells of the rat inner medullary collecting duct. Kidney Int. 31, 1080-1087.

Cousins R.J. and Leinart A.S. (1988). Tissue-specific regulation of zinc metabolism and metallothionein genes by interleukin 1. FASEB J. 2, 2884-2890.

Dehouck B., Fenart L., Dehouck M.-P., Pierce A., Torpier G. and Cecchelli R. (1997). A new function for the LDL receptor: transcytosis of LDL across the blood-brain barrier. J. Cell Biol. 138, 877-889.

Ebadi M. and Sharma S. (2006). Metallothioneins 1 and 2 attenuate peroxynitrite-induced oxidative stress in Parkinson disease. Exp. Biol. Med. 231, 1576-1583.

Feng W., Benz F.W., Cai J., Pierce W.M. and Kang Y.J. (2006). Metallothionein disulfides are present in metallothionein-overexpressing transgenic mouse heart and increase under conditions of oxidative stress. J. Biol. Chem. 281, 681-687.

Fitzgerald M., Nairn P., Bartlett C.A., Chung R.S., West A.K. and Beazley L.D. (2007). Metallothionein-IIA promotes neurite growth via the megalin receptor. Exp. Brain Res. 183, 171-180.

Foulkes E.C. (1978). Renal tubular transport of cadmium-metallothionein. Toxicol. Appl. Pharmacol. 45, 505-512.

Giralt M., Penkowa M., Lago N., Molinero A. and Hidalgo J. (2002a). Metallothionein-1+2 protect the CNS after a focal brain injury. Exp. Neurol. 173, 114-128.

Giralt M., Penkowa M., Hernandez J., Molinero A., Carrasco J., Lago N., Camats J., Campbell I. and Hidalgo J. (2002b). Metallothionein-1+2 deficiency increases brain pathology in transgenic mice with astrocyte-targeted expression of interleukin 6. Neurobiol. Dis. 9, 319-338.

Hamer D.H. (1986). Metallothionein. Annu. Rev. Biochem. 55, 913-951.

Hidalgo J., Penkowa M., Espejo C., Martinez-Caceres E.M., Carrasco J., Quintana A., Molinero A., Florit S., Giralt M. and Ortega-Aznar A. (2006). Expression of metallothionein-I, -II, and -III in Alzheimer disease and animal models of neuroinflammation. Exp. Biol. Med. 231, 1450-1458.

Kagi J.H. and Vallee B.L. (1960). Metallothionein: a cadmium- and zinc-containing protein from equine renal cortex. J. Biol. Chem. 235, 3460-3465.

Kang Y.J., Li G. and Saari J.T. (1999). Metallothionein inhibits ischemia-reperfusion injury in mouse heart. Am. J. Physiol. 276, H993-997.

Kierszenbaum A.L. (2007). Histology and cell biology: an introduction to pathology, 2 ed. Mosby Elsevier. Philadelphia.

Klassen R.B., Crenshaw K., Kozyraki R., Verroust P.J., Tio L., Atrian S., Allen P.L. and Hammond T.G. (2004). Megalin mediates renal uptake of heavy metal metallothionein complexes. Am. J. Physiol. 287, F393-F403.

Klassen R.B., Allen P.L., Batuman V., Crenshaw K. and Hammond T.G. (2005). Light chains are a ligand for megalin. J. Appl. Physiol. 98,

257-263.

Leheste J.-R., Rolinski B., Vorum H., Hilpert J., Nykjaer A., Jacobsen C., Aucouturier P., Moskaug J.O., Otto A., Christensen E.I. and Willnow T.E. (1999). Megalin knockout mice as an animal model of low molecular weight proteinuria. Am. J. Pathol. 155, 1361-1370.

Marino M., Andrews D., Brown D. and McCluskey R.T. (2001). Transcytosis of retinol-binding protein across the renal proximal tubule cells after megalin (gp 330)-mediated endocytosis. J. Am. Soc. Nephrol. 12, 637-648.

Masters B.A., Kelly E.J., Quaife C.J., Brinster R.L. and Palmiter R.D. (1994). Targeted disruption of metallothionein I and II genes increases sensitivity to cadmium. Proc. Natl. Acad. Sci. USA 91, 584-588.

Michalska A.E. and Choo K.H.A. (1993). Targeting and germ-line transmission of a null mutation at the metallothionein I and II loci in mouse. Proc. Natl. Acad. Sci. USA 90, 8808-8092.

Nagano S., Satoh M., Sumi H., Fujimura H., Tohyama C., Yanagihara T. and Sakoda S. (2001). Reduction of metallothioneins promotes the disease expression of familial amyotrophic lateral sclerosis mice in a dose-dependent manner. Eur. J. Neurosci. 13, 1363-1370.

Nilsson S.K., Christensen S., Raarup M.K., Ryan R.O., Nielsen M.S. and Olivecrona G. (2008). Endocytosis of apolipoprotein A-V by members of the low density lipoprotein receptor and the VPS10p domain receptor families. J. Biol. Chem. 283, 25920-25927.

Penkowa M. and Hidalgo J. (2000). Metallothionein I+II expression and their role in experimental autoimmune encephalomyelitis. Glia 32, 247-263.

Penkowa M., Carrasco J., Giralt M., Moos T. and Hidalgo J. (1999). CNS wound healing is severely depressed in metallothionein I- and II-deficient mice. J. Neurosci. 19, 2535-2545.

Richards R.I., Heguy A. and Karin M. (1984). Structural and functional analysis of the human metallothionein-Ia gene: differential induction by metal ions and glucocorticoids. Cell 37, 263-272.

Riedel I.B., Hermans-Borgmeyer I. and Hubner C.A. (2002). SorLA, a member of the LDL receptor family, is expressed in the collecting duct of the murine kidney. Histochem. Cell Biol. 118, 183-191.

Sonn K., Pankratova S., Korshunova I., Zharkovsky A., Bock E., Berezin V. and Kiryushko D. (2010). A metallothionein mimetic peptide protects neurons against kainic acid-induced excitotoxicity. J. Neurosci. Res. 88, 1074-1082.

Spoeglen R., Adams K.W., Koker M., Thomas A.V., Andersen O.M., Hallett P.J., Bercury K.K., Joyner D.F., Deng M., Stoothoff W.H., Strickland D.K., Willnow T.E. and Hyman B.T. (2009). Interaction of the apolipoprotein E receptors low density lipoprotein receptor-related protein and sorLA/LR11. Neuroscience 158, 1460-1468.

Thornalley P.J. and Vasák M. (1985). Possible role for metallothionein in protection against radiation-induced oxidative stress. Kinetics and mechanism of its reaction with superoxide and hydroxyl radicals. Biochim. Biophys. Acta 827, 36-44.

Trendelenburg G., Prass K., Priller J., Kapinya K., Polley A., Muselmann C., Ruscher K., Kannbley U., Schmitt A.O., Castell S., Wiegand F., Meisel A., Rosenthal A. and Dirnagl U. (2002). Serial analysis of gene expression identifies metallothionein-II as major neuroprotective gene in mouse focal cerebral ischemia. J. Neurosci. 22, 5879-5888.

Verroust P.J. and Christensen E.I. (2002). Megalin and cubilin - the story of two multipurpose receptors unfolds. Nephrol. Dial. Transplant. 17, 1867-1871.

Wolff N.A., Abouhamed M., Verroust P.J. and Thevenod F. (2006). Megalin-dependent internalization of cadmium-metallothionein and cytotoxicity in cultured renal proximal tubule cells. J. Pharmacol. Exp. Ther. 318, 782-791.

Wu D. and Pardridge W.M. (1999). Neuroprotection with noninvasive neurotrophin delivery to the brain. Proc. Natl. Acad. Sci. USA 96, 254-259.

Zheng G., Bachinsky D.R., Stamenkovic I., Strickland D.K., Brown D., Andres G. and McCluskey R.T. (1994). Organ distribution in rats of two members of the low-density lipoprotein receptor gene family, gp330 and LRP/alpha 2MR, and the receptor-associated protein (RAP). J. Histochem. Cytochem. 42, 531.

Zlokovic B.V., Martel C.L., Matsubara E., McComb J.G., Zheng G., McCluskey R.T., Frangione B. and Ghiso J. (1996). Glycoprotein 330/megalin: probable role in receptor-mediated transport of apolipoprotein J alone and in a complex with Alzheimer disease amyloid , at the blood-brain and blood-cerebrospinal fluid barriers Proc. Natl. Acad. Sci. USA 93, 4229-4234.

Accepted June 8, 2012